Electrons drift velocity overshot in heterostructures with double-sided donor-acceptor doping and digital barriers

© *A.B. Pashkovskii*[1], *S.A. Bogdanov*[1], *A.K. Bakarov*[2], *K.S. Zhuravlev*[2], *V.G. Lapin*[1], *V.M. Lukashin*[1], *S.N. Karpov*[1], *I.A. Rogachev*[1], *E.V. Tereshkin*[1]

[1] JSC „RPC „Istok" named after Shokin",
141190 Fryazino, Moscow oblast, Russia
[2] Rzhanov Institute of Semiconductor Physics, Siberian Branch, Russian Academy of Sciences,
630090 Novosibirsk, Russia

E-mail: solidstate10@mail.ru

The nonlocal dynamics of electrons in pseudomorphic AlGaAs/GaAs/InGaAs heterostructures with double-sided donor-acceptor doping of AlGaAs barriers and additional digital potential barriers of short-period AlAs/GaAs superlattices around the doped regions has been theoretically studied. For the studied heterostructures, the introduction of digital barriers significantly, by 30−40%, increases the electrons drift velocity overshot when they enter the region of a strong field. The effect of localization of hot electrons on the states in AlAs/GaAs superlattices along the edges of the InGaAs quantum well is revealed. It is shown that taking this effect into account significantly increases the electrons drift velocity overshot, bringing it closer to the maximum theoretical limit for the model used — the drift velocity overshot in the undoped InGaAs bulk material.

Keywords: potential barriers, digital barriers, heterostructures, electrons drift velocity overshot.

1. Introduction

High-power field-effect transistors based on gallium nitride heterostructures have confidently advanced into the millimeter wavelength range in the recent years [1–4]. However, both theoretical studies [5,6] and analysis of the features of the obtained record results [4] show that it will be difficult to move up the frequency range for devices based on gallium nitride without fundamentally new technical solutions. The situation is exactly opposite for heterostructures based on gallium arsenide: gallium arsenide pseudomorphic heterostructures have great potential to improve parameters, especially in terms of operating frequencies. One of the main directions — increasing the effective depth of the quantum well (QW) of the channel. It can be achieved in different ways: both by directly increasing the gap of zones at the boundary of the heterojunction [7], and by using various narrow-band inserts into the quantum well [8]. Another way to improve the characteristics is to use a spacer in the form of an AlAs/GaAs [9] superlattice, which leads to an increase in the mobility of a two-dimensional electron gas (2DEG) either due to a decrease in the spreading width of the δ-layer [10], or due to screening of the scattering potential of impurities by electrons in the X-valleys of the AlAs layers of the spacer [11] or a decrease in the degree of hybridization of electron wave functions in the QWs and in the donor region [12]. At the same time, 2DEG concentration can decrease both due to the difficulty of tunneling from donors to QWs through a higher barrier, and the capture of part of the electrons to the states of

the X-valley of AlAs layers. This, in turn, can result in a decrease of the conductivity of the heterostructure.

In addition, the effective depth of the quantum well can be increased by using sharp donor-acceptor doping along the edges of the channel [13]. This method turned out to be very effective and allowed for obtaining a number of record results for transistors of the centimeter wavelength range [14]. Undoubtedly, an effective combination of these methods is possible [15]. In addition, with donor-acceptor doping, another way to increase the effective depth of the quantum well is possible — using a set of thin (several atomic monolayers) AlAs barriers with gaps of several GaAs monoatomic layers not only in the spacer, but also in the interval between $n-\delta$ by layer and acceptors. Barriers made of short-period AlAs/GaAs superlattices allow for obtaining smoother QW boundaries and reduce the concentration of impurities in QWs by catching them at heterogrammes. The arrangement of δ-silicon layers in GaAs layers allows for achieving a greater doping efficiency and reducing the number of deep traps in structures [16]. In addition, the capture of cold electrons to the states of the X-valley of AlAs/GaAs superlattices, where their mobility is low, is unlikely due to high energy even of the first level of a superlattice with thin layers of AlAs. Due to these effects, superlattice barriers are widely used to create quantum wells with a highly mobile two-dimensional electron gas [17]. Such barriers are often called digital by analogy with the binary digital code. Heterostructures with such barriers allowed for obtaining transistors with very high gain [18].
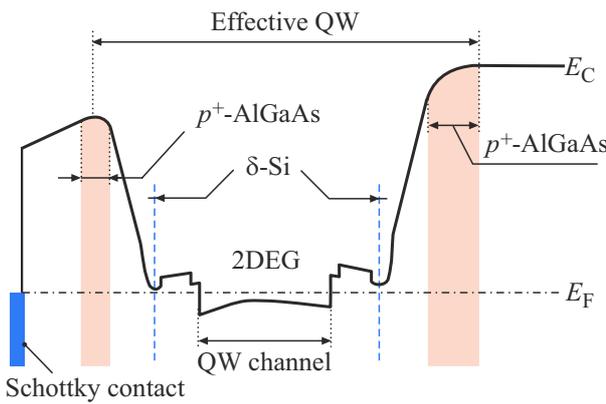
Figure 1. Schematic representation of the energy band diagram DA-DpHEMT of the heterostructure. The positions of the layers with doping donors and acceptors are shown.

2. Structural features of heterostructures with digital barriers

Fig. 1 shows an AlGaAs/GaAs/InGaAs energy band diagram of a pseudomorphic heterostructure with bilateral channel doping and additional potential barriers (DA-DpHEMT).

The main problem of traditional heterostructures for high-power transistors — strong real space transfer transfer of electrons from the InGaAs channel to the AlGaAs barriers when a strong electric field is applied along the channel [15]. This leads to strong delocalization and a drop in electron mobility in a strong field due to intense scattering in AlGaAs barriers. With donor-acceptor doping of AlGaAs barriers, sharp $p-i-n$ potential barriers are formed on both sides of the InGaAs channel of the heterostructure. This significantly increases the degree of localization of electrons in the channel, and thus, due to the suppression of real space transfer, it noticeably increases both the drift velocity of electrons [19] and its overshot when electrons enter the region of a strong field (under the gate of the transistor) [15,20].

All these effects strongly depend both on the gap of zones at the boundary of the heterostructure, and on the effectiveness (sharpness and height) of additional barriers [15]. At the same time, the size of the zone gap is determined by the choice of a heteroparticle, and the potential profile of additional barriers is determined by technological limitations with respect to the surface density of donors in the $n-\delta$-layer. In addition, with an increase in the surface density of donors in the δ-layer, the scattering of electrons in the channel increases and their mobility decreases. However, as noted above, in the heterostructure, short-period AlAs/GaAs superlattices consisting of thin (two to six monolayers) layers of [16–18] can be used instead of homogeneous materials. The gap in the conduction band at the heterogeneous boundaries between the InGaAs channel and the AlAs/GaAs superlattice will obviously be

larger than the gap at the heterogeneous boundary of the InGaAs channel and a homogeneous AlGaAs solid solution with a composition close to the averaged composition of the superlattice. This can increase the localization of hot electrons in the channel.

3. Description of the calculation model

The transport characteristics of the DA-DpHEMT heterostructure in a strong electric field were calculated on the basis of a phenomenological model designed to analyze the nonlocal heating of electrons in transistor heterostructures with an idealized (infinitely long) gate with strong dimensional quantization in the direction perpendicular to the surface of the structures [15]. Within the framework of this model, the potential relief and the levels of dimensional quantization for this direction are determined on the basis of a numerical self-consistent solution of the Schrodinger and Poisson equations:

$$-\frac{\hbar^2}{2}\frac{d}{dx}\left(\frac{1}{m^*(x)}\frac{d\Psi_i(x)}{dx}\right)$$
$$+\left(E_{c0}(x)-q\cdot\varphi(x)\right)\Psi_i(x)=E_i\Psi_i(x),$$
$$\frac{d}{dx}\left(\kappa(x)\frac{d\varphi(x)}{dx}\right)=-\frac{\rho(x)}{\kappa_0}. \qquad (1)$$

Hereinafter $\Psi_i(x)$ and E_i —eigenfunctions and eigenvalues of the Hamilton operator, $E_{c0}(x)$ — a function that defines the profile of potential energy differences corresponding to the electric the potential of the bottom of the conduction band in the absence of free charges, q — the absolute value of the electron charge, $\rho(x)$, $\varphi(x)$ — the density and potential of the spatial charge, $\kappa(x)$, κ_0 — dielectric constant of a semiconductor and vacuum, m^* — effective mass of an electron in the conduction band, $\hbar$ — Planck's constant.

A significant difference in the structure under consideration is the addition of a large number of thin, high AlAs barriers near the InGaAs channel, whereas only heterojunctions at the channel boundaries were considered in [15]. In regions of coordinate space where the bottom of the conduction band is above the last found level, the energy spectrum is considered continuous, and the volume charge density is calculated using the formulas:

$$\rho(x)=q(N_D(x)-N_A(x))+\rho_c(x),$$
$$\rho_c(x)=-qn_c(x)$$
$$=-q\cdot N_c(x)\cdot\int_0^\infty\frac{\sqrt{E_k}dE_k}{1+\exp\left(\frac{E_k-E_F}{kT}\right)}, \qquad (2)$$

where $N_c(x)=2\left(\frac{2\pi m^*(x)kT}{(2\pi\hbar)^2}\right)^{3/2}$ — effective density of states in the conduction band, $N_D(x)$ and $N_A(x)$ — concentrations of ionized donors and acceptors, E_k —

electron energy in the conduction band, E_F — Fermi energy, k — Boltzmann constant, T — absolute temperature.

In the region of space where the wave functions of the discrete energy spectrum are localized E_i (quantum domain):

$$\rho(x) = q\left(N_D(x) - N_A(x)\right) + \rho_c(x) - q\sum_i n_i |\Psi_i(x)|^2,$$

$$n_i = \left(\frac{m^*(x)kT}{\pi\hbar^2}\right)\ln\left\{1 + \exp\left[\frac{E_F - E_i}{kT}\right]\right\}. \qquad (3)$$

In the direction parallel to the surface of the structure, electron transport is described on the basis of a phenomenological system of momentum and energy conservation equations [15] with relaxation times for bulk materials [21]. This system assumes that the electron scattering frequency is given in the form

$$\nu = \nu_1 p_1 + \nu_2 p_2, \qquad (4)$$

where p_1, p_2, ν_1, ν_2 — probabilities of occurrence of electrons and their the scattering frequencies in the narrow-band channel layer and in the wide-band layers framing the channel, respectively, are noted as

$$m^*(\varepsilon) = m_1^*(\varepsilon)p_1 + m_2^*(\varepsilon)p_2, \qquad (5)$$

$$\frac{\partial\left(m^*(\varepsilon)V\right)}{\partial t} =$$

$$= q\left(E - \frac{m^*(\varepsilon)V\left(m_1^*(\varepsilon)V_{s1}(\varepsilon)E_{s2}(\varepsilon)p_2 + m_2^*(\varepsilon)V_{s2}(\varepsilon)E_{s1}(\varepsilon)p_1\right)}{m_1^*(\varepsilon)V_{s1}(\varepsilon)m_2^*(\varepsilon)V_{s2}(\varepsilon)}\right), \qquad (6)$$

$$V_s(E) =$$

$$= \frac{m_1^*(E)V_{s1}(E)m_2^*(E)V_{s2}(E)}{\left(m_1^*(E)p_1 + m_2^*(E)p_2\right)\left(m_1^*(E)V_{s1}(E)p_2 + m_2^*(E)V_{s2}(E)p_1\right)}, \qquad (7)$$

$$\frac{\partial\varepsilon}{\partial t} = q\left(EV - V_s(\varepsilon)\left(E_{s1}(\varepsilon)p_1 + E_{s2}(\varepsilon)p_2\right)\right). \qquad (8)$$

Here q, V, m^*, $\varepsilon = 3kT/2$ — charge, velocity, averaged effective mass and electron energy, respectively, E — electric field strength, $V_{si}(\varepsilon)$, $E_{si}(\varepsilon)$ — static values of the electron drift velocity and electric field strength corresponding to the specified energy ε obtained from Monte Carlo calculations of the static characteristics of materials [22].

Both systems are solved in a self-consistent manner to describe the dynamics of electrons. The response of the drift velocity and the probability of occurrence of electrons in a wide-band material to an electric field pulse with an amplitude approximately equal to the average value of the field under the gate of a millimeter-wavelength transistor is sought. The relationship of the magnitude of the electric field strength and time was set as follows: during 0.2 ps, electrons move in a field with a strength of 1 kV/cm, then a pulse with an amplitude of 20 kV/cm with a duration of 1 ps is applied, after which the electron drift continues in an electric field with a strength of 1 kV/cm.

During the movement in a strong inhomogeneous electric field, the temperature of the electron gas changes noticeably, which significantly affects the occupancy levels in the QW — channel of the transistor. At first glance, the occupation of the levels in the QW depends only on the temperature of the electron gas, as in the state of thermodynamic equilibrium, however, this approximation is valid only if the overlap integrals of the wave functions at the QW levels are large enough and electrons can quickly move between them. This condition is met for the structures of the first and second types considered in [15], while structures with digital barriers can have situations when such an approximation is unfair, which leads to very interesting consequences.

Naturally, such a simple model does not allow for taking into account a number of subtle moments, for example, the change in the scattering intensity associated with the quantization of electrons in a wide range of energies, and the difference between wave functions in a narrow quantum well from wave functions in the volume, scattering at heterogrammes, etc., etc. Of course, for a more accurate description, it is desirable to solve the kinetic equation, which correctly takes into account all the changes in the scattering mechanisms associated with the quantization of levels and the shape of the potential well. However, so far only the first steps are taken in this direction [23].

4. Calculation results

Let's consider three types of heterostructures used for the production of high-power field-effect transistors with a Schottky barrier, shown in Fig. 2. The first — is a traditional, widely used worldwide heterostructure of the type $Al_xGa_{1-x}As/In_yGa_{1-y}As/Al_xGa_{1-x}As$ with two-sided $\delta-n$-doping (DpHEMT), in which due to technological restrictions the molar fraction of aluminum usually does not exceed 30% ($x < 0.3$), and the molar fraction of indium $y < 0.2$ (Fig. 2, a). The second — is a similar structure with additional potential barriers at the edges of the quantum well based on sharp $p-i-n$ transitions (Fig. 2, b). It is exactly such structures, due to the suppression of real space electron transfer, which have made it possible to almost double the gain coefficient and the specific power of transistors based on them [14]. The third — is a structure with AlAs/GaAs superlattices around δ-layers, used in [18] for the manufacturing of millimeter-wave transistors (Fig. 2, c). Taking into account further calculation results, such a structure can be called Q-DpHEMT (quantum DpHEMT).

It can be seen that in all three cases, the degree of localization of electrons in the quantum well differs significantly. As noted earlier [15], the weakest electrons are localized in the channel region in the traditional DpHEMT structure (Fig. 2, a). Their localization in the DA-DpHEMT
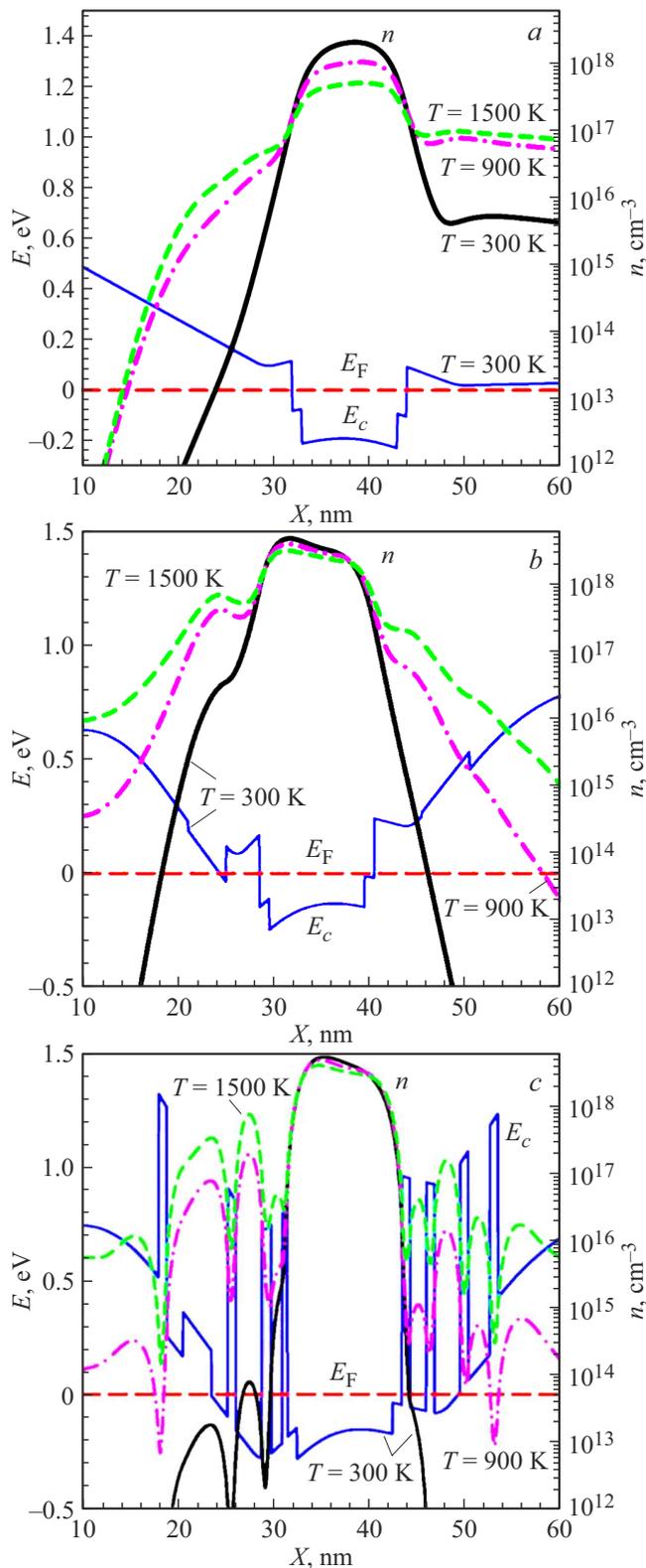
Figure 2. AlGaAs/InGaAs/GaAs energy band diagrams of heterostructures and electron concentration distribution at different electron gas temperatures: *a* — traditional D*p*HEMT, *b* — structure with donor-acceptor doping (DA-D*p*HEMT), *c* — a structure with donor-acceptor doping and additional potential barriers from AlAs/GaAs superlattices (Q-D*p*HEMT). (A color version of the figure is provided in the online version of the paper).
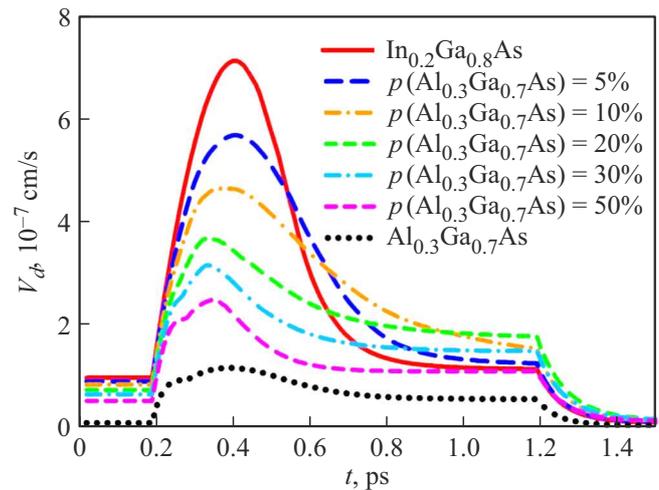
Figure 3. The dependencies of the electron drift velocity on time when electrons fly into the region of a strong field ($t < 0.2$ ps, $E = 1$ kV/cm; 0.2 ps$< t < 1.2$ ps, $E = 20$ kV/cm; $t > 1.2$ ps, $E = 1$ kV/cm) with a different given probability of their being in the wide-band $Al_{0.3}Ga_{0.7}As$-barrier outside the channel — $p(Al_{0.3}Ga_{0.7}As)$.

structure (Fig. 2, *b*) is noticeably stronger. Hot electrons are localized even more strongly in a heterostructure with digital barriers (Fig. 1, *c*).

To demonstrate the relevance of these differences more clearly, Fig. 3 shows the dependencies of the electron drift velocity on time when they fly into the strong field region for various probabilities of occurrence of electrons in the wide-band $Al_{0.3}Ga_{0.7}As$-barrier. In this case, when solving a system of hydrodynamic equations, the probability of occurrence of electrons outside the channel was simply set, and not determined from solving the self-consistent Schrodinger and Poisson equations. It can be seen that the magnitude of the electron drift velocity overshot when flying into the strong field region strongly depends on the number of electrons in the wide-band material. So, the overshot of the drift velocity drops by 1.5 times with only 10% probability of occurrence in a wide-band material.

The dependencies of the drift velocity of electrons and their probability of occurrence in a wide-band material on the time when the electrons enter the region of a strong field are shown on Fig. 4 for the structures considered above.

As expected, the smallest overshot in drift velocity is observed in the traditional D*p*HEMT structure. The probability of occurrence of electrons outside the QW in a strong field is maximal for this structure. In the D*p*HEMT structure, the probability of occurrence of electrons outside the QW in a weak field is less than in the DA-D*p*HEMT structure due to a ~ 1.5 times lower surface electron density. For the same reason, the drift velocity overshot in these structures differs less than in the structures considered earlier in [15]. It can also be seen that the introduction of digital barriers, even quite

randomly, greatly reduces the probability of transitions to wide-band material, which leads to a significant (by $\sim 40\%$) increase of the drift velocity. In fact, this difference explains the unusually high gain coefficients of the transistors provided in [18].

Obviously, the design of the Q-DpHEMT structure can be improved by inserting additional digital barriers. Figure 5 shows a variant of the structure in which thick layers of Al$_x$Ga$_{1-x}$As between the channel and the gate are replaced by digital superlattices of three AlAs monolayers and six GaAs monolayers. On average, the molar fraction of aluminum in superlattices is approximately $x = 0.3$. Figure 5 shows an energy band diagram of such a structure and quantum levels in it at the temperature of an electron gas $T = 1500$ K (the wave functions of electrons at the third and fifth quantum levels are localized in the channel and are not given so as not to clutter the figure, the Fermi level and the first quantum level in the scale of the figure practically coincide).
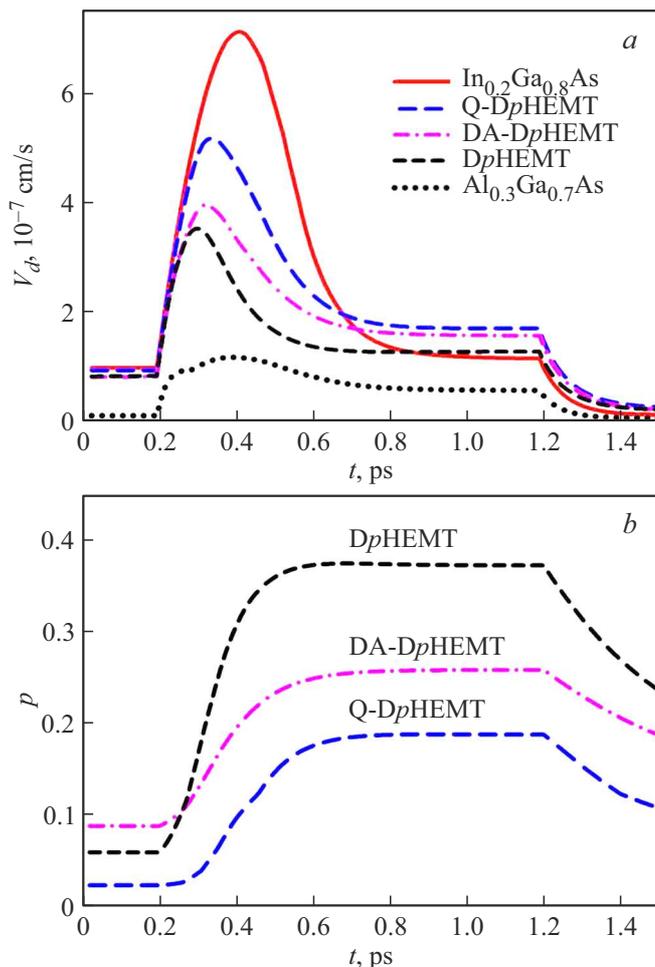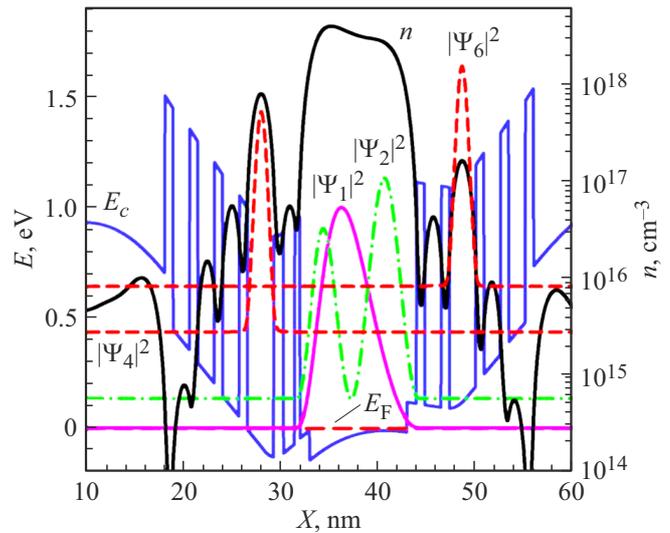
Figure 5. Energy band diagram, squares of electron wave functions at corresponding quantum levels, electron concentration distribution.

This structure has one interesting feature. A sufficiently high concentration of donors is needed to make DA-DpHEMT structures in δ-layers, and for this, the GaAs matrix layers around the δ-layer should be thick enough (at least 4 monolayers), otherwise the mobility of electrons decreases, which was observed experimentally. In addition, the local minima of the Coulomb potential occur exactly on the δ-layers. This leads to the fact that energy „gaps" with localized electronic states are produced in an almost ideal superlattice, probably due to an increase in the distance between the barriers and the local minimum of the Coulomb potential. The fourth and sixth quantum levels are such localized states for this structure. The electrons are rigidly localized on them outside the channel in the area of digital barriers (see Fig. 5), and their wave function in the channel region is almost zero.

Localization of electrons outside the channel should lead to another extremely interesting and useful effect for microwave transistors. Since these quantum levels are quite high, when electrons move in a weak electric field in a state close to thermodynamic equilibrium with a low temperature of the electron gas, these levels are not occupied. Electrons move almost ballistically [24] in the region of a strong electric field under the short gate of a millimeter-wavelength transistor. The electrons do not manage to pass to these levels within a short time of the flight of electrons under the gate of the transistor since the matrix element of the transition, and therefore the probability of transition is small. Which in turn should dramatically reduce the probability of scattering in a wide-band material. The results of the calculation of the drift velocity overshot, both taking into account the population of all levels and taking into account the effect described above, are shown in Fig. 6. In this calculation the levels

Figure 4. The dependencies of the drift velocity of electrons (a) and the probability (b) of their occurrence in a wide-band material on the time when electrons fly into the region of a strong field ($t < 0.2$ ps, $E = 1$ kV/cm; 0.2 ps $< t < 1.2$ ps, $E = 20$ kV/cm; $t > 1.2$ ps, $E = 1$ kV/cm).
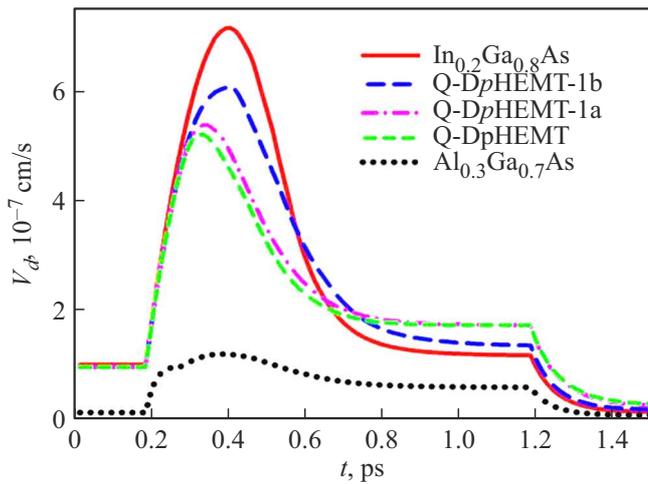
Figure 6. The dependencies of the electron drift velocity when electrons fly into the region of a strong field ($t < 0.2\,\mathrm{ps}$, $E = 1\,\mathrm{kV/cm}$; $0.2\,\mathrm{ps} < t < 1.2\,\mathrm{ps}$, $E = 20\,\mathrm{kV/cm}$; $t > 1.2\,\mathrm{ps}$, $E = 1\,\mathrm{kV/cm}$).

with localized states simply were not taken into account in calculation. Here Q-DpHEMT — structure corresponding to Fig. 2, c; Q-DpHEMT-1, a: structure corresponding to Fig. 5, Q-DpHEMT-1, b: the same structure — calculation taking into account the localization of electrons in the barrier lattice.

It can be seen that the introduction of additional barriers slightly increases the drift velocity overshot of the electron, and taking into account the occurrence of localized states leads to a further very significant increase in the overshot of the drift velocity.

The issue with large gaps between barriers in the $\delta - n$ area of the layer can be solved in a fairly simple way. δ the layer can be split into two, simultaneously reducing the size of the GaAs matrix, for example, to two monolayers on each side, and a barrier of three AlAs monolayers can be placed between them. If we reduce the distance between the other barriers to four GaAs monolayers, we will get an almost ideal superlattice (see Fig. 7). Here the temperature of the electron gas is $T = 1500\,\mathrm{K}$. The wave function of electrons at the fourth quantum level is localized in the channel and is not shown so as not to clutter the drawing.

In such a structure, electrons are localized in the channel even more strongly than in the previous one, and significant delocalization begins only from the fifth level with an energy of $> 0.6\,\mathrm{eV}$. As a result, a drift velocity overshot in such a structure (see Fig. 7), both taking into account and without taking into account the states localized in the superlattice, approaches the theoretical limit for this model — a drift velocity overshot in the bulk material of the channel. Fig. 8 Q-DpHEMT-2, a: shows a structure with a short superlattice AlAs/GaAs, Q-DpHEMT-2, b: the same structure — calculation taking into account the localization of states in the barrier lattice.

Another feature of the structure under consideration should be noted. The distances between the first ($-0.065\,\mathrm{eV}$) and second levels ($0.062\,\mathrm{eV}$) filled in the equilibrium state, and even more so the third ($0.289\,\mathrm{eV}$) and fourth ($0.580\,\mathrm{eV}$) are very large, significantly more energy of the optical phonon. This can reduce the probability of electron scattering on optical phonons, which should further increase in the drift velocity overshot, and therefore significantly increase the operating frequencies of field-effect transistors based on these heterostructures.
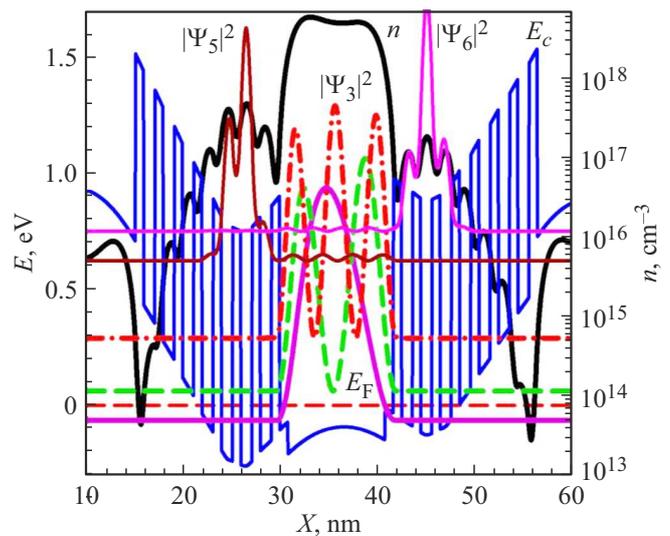
Figure 7. Energy band diagram, squares of electron wave functions at corresponding quantum levels, electron concentration distribution.
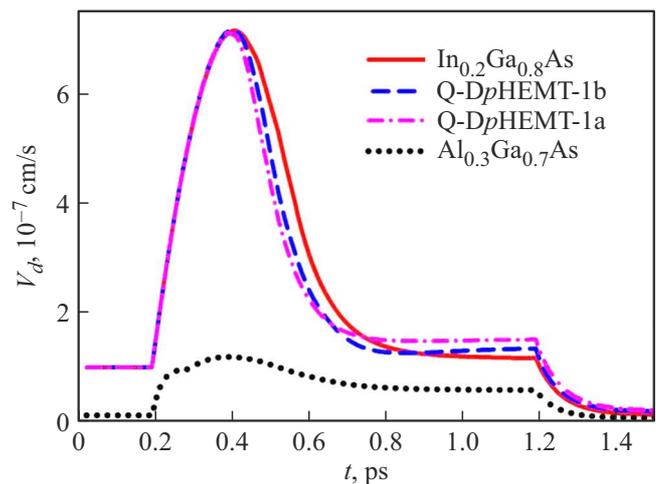
Figure 8. The dependencies of the electron drift velocity when electrons enter the strong field region in a structure with ideal short-period superlattices at the edges of the channel ($t < 0.2\,\mathrm{ps}$, $E = 1\,\mathrm{kV/cm}$; $0.2\,\mathrm{ps} < t < 1.2\,\mathrm{ps}$, $E = 20\,\mathrm{kV/cm}$; $t > 1.2\,\mathrm{ps}$, $E = 1\,\mathrm{kV/cm}$). Q-DpHEMT-2, a calculation without taking into account localization of states in lateral superlattices, Q-DpHEMT-2, b — calculation taking into account the localization of states.

5. Conclusion

The results obtained show that the use of digital barriers in heterostructures with donor-acceptor doping is a very effective way to improve transistor heterostructures.

It is theoretically demonstrated that when digital barriers are introduced into AlGaAs/InGaAs/GaAs heterostructures selectively doped with donors and acceptors with a two-dimensional electron gas, two new quantum effects are manifested that have a significant positive effect on the transport characteristics of structures in a strong electric field. Firstly, the localization of hot electrons in a quantum well, even under conditions of thermodynamic equilibrium, is noticeably stronger than in structures without digital barriers. This results in a noticeable decrease of scattering in the barriers of the quantum well, which in turn leads to a noticeable (up to 50%) increase in the drift velocity overshot of electrons when they enter the region of a strong field. Secondly, the localization of electronic states at some excited quantum levels inside the area of digital barriers near the quantum well can lead to the fact that the time of flight of hot electrons across this region will not be sufficient for their transition to these levels. The probability of occurrence of electrons outside the channel with high mobility will decrease, which in turn leads to an additional significant increase of the drift velocity overshot.

The optimization of heterostructures leads to a further increase of the drift velocity overshot, bringing it closer to the theoretical limit for the model under consideration, — a drift velocity overshot in the bulk material of the quantum well.

Devices with such structures can have a gain up to 2 times higher, while maintaining other high parameters unchanged, for example, specific power. A number of parameters of field-effect transistors based on such structures can compete with gallium nitride-based devices and transistors with a channel based on $In_xGa_{1-x}As$ with a high molar content of indium, especially in the millimeter and submillimeter wavelength ranges.

Conflict of interest

The authors declare that they have no conflict of interest.

References

[1] H. Wang, F. Wang, S. Li, T.Y. Huang, A.S. Ahmed, N.S. Mannem, J. Lee, E. Garay, D. Munzer, C. Snyder, S. Lee, H.T. Nguyen, M.E.D. Smith. (Jul. 2019). Power Amplifiers Performance Survey 2000-Present. [Online]. Available: https://gems.ece.gatech.edu/PA_survey.html

[2] B. Romanczyk, S. Wienecke, M. Guidry, H. Li, E. Ahmadi, X. Zheng, S. Keller, U.K. Mishra. IEEE Trans. Electron Dev., **65** (1), 45(2018).

[3] N.S. Dasgupta, S. Keller, J.S. Speck, U.K. Mishra. IEEE Electron Dev. Lett., **32** (12), 1683 (2011).

[4] Y. Tang, K. Shinohara, D. Regan, A. Corrion, D. Brown, J. Wong, A. Schmitz, H. Fung, S. Kim, M. Micovic. IEEE Electron Dev. Lett., **36** (6), 549 (2015).

[5] B.E. Foutz, S.K. O'Leary, M.S. Shur, L.F. Eastman. J. Appl. Phys., **85** (11), 7727 (1999). DOI: 10.1063/1.370577

[6] S.A. Bogdanov, A.A. Borisov, S.N. Karpov, M.V. Kuliyev, A.B. Pashkovsky, E.V. Tereshkin. Tech. Phys. Lett., **48** (2), 44 (2022).

[7] I.S. Vasilevsky, A.N. Vinichenko, N.I. Kargin. Tez. dokl. 8-y Mezhdunar. nauch.-prakt. konf. po fizike i tekhnologii nanogeterostrukturnoi SVCh-elektroniki. (Mokerovskie Chteniya, May 24, Moscow) p. 28. (in Russian).

[8] D.S. Ponomarev, I.S. Vasilevsky, G.B. Galiev, E.A. Klimov, R.A. Khabibullin, V.A. Kulbachinsky, N.A. Yuzeeva. FTP, **46** (4), 500 (2012). (in Russian).

[9] D.A. Safonov, A.N. Vinichenko, N.I. Kargin, I.S. Vasilevsky. Tech. Phys. Lett., **44** (4), 34 (2018).

[10] K. Inoue, H. Sakaki, J. Yoshino, Y. Yoshioka. Appl. Phys. Lett., **46**, 9735 (1985).

[11] K.-J. Friedland, R. Hey, H. Kostial, R. Klann, K. Ploog. Phys. Rev. Lett., **77**, 4616 (1996).

[12] A.N. Vinichenko, V.P. Gladkov, N.I. Kargin, M.N. Strikhanov, I.S. Vasilevsky. FTP, **48** (12), 1660 (2014).

[13] K.S. Zhuravlev, D.Yu. Protasov, D.V. Gulyaev, A.K. Bakarov, A.I. Toropov, V.G. Lapin, V.M. Lukashin, A.B. Pashkovski. Adv. Microelectron.: Rev., v. 2 (Barcelona, Spain: IFSA, 251 (2019).

[14] V.M. Lukashin, A.B. Pashkovsky, K.S. Zhuravlev, A.I. Toropov, V.G. Lapin, A.B. Sokolov. Tech. Phys. Lett., **38** (17), 84 (2012).

[15] A.B. Pashkovsky, A.S. Bogdanov, V.M. Lukashin, S.I. Novikov. Mikroelektronika, **49** (3), 210 (2020) (in Russian).

[16] T. Baba, T. Mizutani, M. Ogawa. Jpn. J. Appl Phys., **22**, L627e9 (1983).

[17] T. Sajoto, M. Santos, J.J. Heremans, M. Shayegan, M. Heiblum, M.V. Weckwerth, U. Meirav. Appl. Phys. Lett., **54**, 840 (1989).

[18] A.B. Pashkovskii, S.A. Bogdanov, A.K. Bakarov, A.B. Grigorenko, K. S. Zhuravlev, V.G. Lapin, V.M. Lukashin, I.A. Rogachev, E.V. Tereshkin, S.V. Shcherbakov. IEEE Trans. Electron Dev., **68** (1), 53 (2021).

[19] D.Yu. Protasov, D.V. Gulyaev, A.K. Bakarov, A.I. Toropov, E.V. Erofeev, K.S. Zhuravlev. Tech. Phys. Lett., **44** (6), 77 (2018).

[20] A.A. Borisov, K.S. Zhuravlev, S.S. Zyrin, V.G. Lapin, V.M. Lukashin, A.A. Makovetskaya, V.I. Novoselets, A.B. Pashkovsky, A.I. Toropov, N.D. Ursulyak, S.V. Shcherbakov. Tech. Phys. Lett., **42** (16), 41 (2016).

[21] M. Shur. Electron. Lett., **12** (23), 615 (1976).

[22] A.V. Garmatin. Elektron. tekhn., ser. 1. Elektronika SVCh., **3** (377), 66 (1985) (in Russian).

[23] D.Yu. Protasov, K.S. Zhuravlev. Solid-State Electron., **129**, 66 (2017).

[24] A. Cappy, B. Carnez, R. Fauquembergues, G. Salmer, E. Constant. IEEE Trans. Electron Dev., **27** (11), 2158(1980).

Translated by A.Akhtyamov